



Evaluation of Liquefaction Potential based on Cone Penetration Test (CPT) and Semi-empirical Methods

Fatima Ezzahraa Latifi ^{1*}, Khadija Baba ², Ghizlan Ardouz ¹, Latifa EL Bouanani ²

¹ Civil Engineering, Water, Environment and Geosciences Centre (CICEEG), Mohammadia School of Engineering, Mohammed V University, Rabat, Morocco.

² Civil Engineering and Environment Laboratory, High School of Technology-Salé, Mohammed V University, Rabat, Morocco.

Received 08 November 2022; Revised 16 January 2023; Accepted 25 January 2023; Published 01 February 2023

Abstract

The phenomenon of soil liquefaction can be an induced effect of earthquake shaking where the saturated soil loses some or all of its bearing capacity and stiffness. Likewise, the increase of water pressure in the soil pores under the seismic wave causes a decrease of the shear strength. As a result, the soil becomes liquefied and susceptible to producing permanent deformations. The phenomenon of liquefaction is generally unpredictable, and neglecting it can influence the stability of structures and infrastructure foundations. Since the 1964 Alaska and Niigata earthquakes, more research works have been conducted to assess land liquefaction vulnerability. This study is undertaken in this field, whose objective, on the one hand, is to signal the phenomenon of liquefaction in the north of Morocco as a geo-technical part known for its instability and, on the other hand, to study the semi-empirical methods to adequately evaluate the liquefaction potential while specifying the most appropriate method for our case study. Similarly, the study is based on data derived from experimental results of in-situ tests applied to the embankment crossing the valley of "Oued Gharifa" on a high-speed rail line section from KP 228+400 to KP 229+375. Moreover, this research aims to show and discuss the evaluation of liquefaction potential of the experimental results of the CPT (cone penetration test) using three semi-empirical methods, namely the Juang method, the Olsen method, and the Robertson method. In doing so, we are going to compare the application results of the three semi-empirical methods in light of evaluating the liquefaction likelihood of the studied area, taking into account the nature of the soil, the variation of the safety coefficient, and the liquefaction potential for each method as well.

Keywords: Liquefaction, Semi-Empirical Methods, Earthquake, Liquefaction Potential, CPT.

1. Introduction

Soil liquefaction is one of the most dangerous phenomena that generally affects saturated, powdery soils. Under earthquake shaking and undrained conditions, the soil loses some or all of its bearing capacity. This loss is due to increasing pressure in soil pores, which leads to effective stress diminution where the soil can no longer resist the shear forces. Hence, the soil liquefaction causes enormous deformations that directly influence the stability of a structure's foundation and infrastructure. Historically, the economic and human damages caused by the earthquakes in Niigata and Alaska in 1964 [1–3] pushed researchers around the world to develop approaches for understanding the liquefaction risk. Consequently, several semi-empirical methods have been developed through theoretical considerations and experimental results, especially in-situ test results.

* Corresponding author: fatimaezzahraa_latifi@um5.ac.ma

 <http://dx.doi.org/10.28991/CEJ-2023-09-02-013>



© 2023 by the authors. Licensee C.E.J, Tehran, Iran. This article is an open access article distributed under the terms and conditions of the Creative Commons Attribution (CC-BY) license (<http://creativecommons.org/licenses/by/4.0/>).

These methods are organized into three main families, namely, the cyclic deformation approach [4, 5], the energy approach [6] and the cyclic stress approach [7–11]. The study is based predominantly on the most developed and practically used approach, i.e., the cyclic strain approach, seen as the estimation of the ratio of cyclic strain to cyclic resistance [12–14].

At the beginning, these approaches were based on laboratory tests like the triaxial test so as to study the movement of the soil which requires transferring the samples to the laboratory; a process whereby their original and natural state might know such impact. For this reason, the evaluation of liquefaction potential is based on the in-situ tests, mainly the CPT test (cone penetration test) [8, 15] and the SPT test (dynamic penetrometer test) [16], where the semi-empirical methods are meant to relate the latter with historical cases in order to obtain a relation giving an increase in pressure in the pore as a function of earthquake magnitude.

Within this context, this article is established in two parts and aims to first explain the liquefaction phenomenon using semi-empirical methods applied in evaluating liquefaction potential in order to give importance to this phenomenon in Morocco as a country known for its geological and geotechnical particularities. Then, investigate the susceptibility of liquefaction in the compressible area of the valley of Oued Gharifa to realize the section of the high-speed line from KP 228+400 to KP 229+375 in the northwest of Morocco. Furthermore, the semi-empirical methods used in this paper are considered to be part of the cyclic stress approach and are based on the results of the cone penetration tests (CPT), particularly the Olsen method [8, 17], the Robertson method [9, 18], and the Juang method [7, 19].

2. Semi-Empirical Methods for the Estimation of Liquefaction Potential

Nowadays, there are various semi-empirical methods to determine the liquefaction susceptibility of a soil, which is quantified by a liquefaction potential. This potential represents the soil's ability to resist under seismic stress, to put it differently, it depends mainly on the type of soil, particle shape (granulometry), relative density, degree of saturation, and the magnitude of the earthquake. Semi-empirical methods have been established through the observation of earthquake histories as well as the results of in-situ tests. Accordingly, these methods could be classified into three approaches:

- Cyclic stress approach;
- Cyclic deformation approach;
- Energy approach.

Above all, the evaluation of the liquefaction potential was made via laboratory tests in order to analyze the response of soil to earthquakes. This action, subsequently, changes the structure and texture of the soil and results in a direct influence on resistance to liquefaction. For this reason, in-situ tests are the most commonly used to estimate the potential for liquefaction. As a matter of fact, not only the static penetrometer test (CPT) and the dynamic penetrometer test (SPT) allow us to obtain intact samples but also the mechanical characteristics of the soil. Regarding these ideas, we are going to emphasize the cyclic stress approach, which represents the soil response to earthquake solicitations, by calculating the safety factor (F_s), which is defined as the ratio of the cyclic resistance CRR to the cyclic stress CSR (Equation 1) [20, 21]:

$$F_s = CRR/CSR \quad (1)$$

2.1. Evaluating Cyclic Resistance (CRR)

2.1.1. Olsen Method

It is to mention that Olsen et al has facilitated the estimation of the CRR considering the evaluation of the CRR1 which represents the normalized cyclic liquefaction resistance ratio. Also, considering the results from the CPT test, chiefly, q_c representing the tip resistance and f_s the sleeve friction resistance, CRR1 is given as follows:

$$CRR1 = 0.00128 \left(\frac{q_c}{\sigma'_{v0}} \right)^{0.7} - 0.025 + 0.17R_f - 0.028R_f^2 + 0.0016R_f^3 \quad (2)$$

where σ'_{v0} is the effective stress and R_f is the rational fiction. Fiction ration is expressed as follows:

$$R_f = \frac{f_s}{q_c} \times 100 \quad (3)$$

Subsequently, the cyclic resistance ratio CRR can be determined with reference to CRR_1 ratio, therefore the effect of the in-situ vertical effective stress and the magnitude of the earthquake CRR is given as the following:

$$CRR = CRR_1 \times MSF \times K\sigma \times K\alpha \quad (4)$$

where MSF is the estimated magnitude scale factor, $K\sigma$ is the stress factor for confinement scaling, it adjusts the failure envelope curvature from liquefaction strength to the vertical effective stress envelope [22-24], and $K\alpha$ is the Scale factor of initial shear stress.

2.1.2. Juang Method

According to Juang et al, the cyclic strength ratio can be evaluated as follows:

$$CRR = C_\sigma \exp \left[-2.957 + 1.264 \left(\frac{q_{c1N,cs}}{100} \right)^{1.25} \right] \quad (5)$$

where C_σ is given as the following

$$C_\sigma = -0.016 \left(\frac{\sigma'_{v0}}{100} \right)^3 + 0.178 \left(\frac{\sigma'_{v0}}{100} \right)^2 - 0.063 \left(\frac{\sigma'_{v0}}{100} \right) + 0.903 \quad (6)$$

$$K_I = 2.249(I_c)^4 - 16.943(I_c)^3 + 44.551(I_c)^2 - 51.497(I_c) + 22.802 \quad (7)$$

$$I_c = [(3.47 - \log_{10} q_{c1N})^2 + (\log_{10} F + 1.22)^2]^{0.5} \quad (8)$$

F is normalized friction ratio defined as:

$$F = \frac{f_s}{(q_c - \sigma_v)} \times 100 \quad (9)$$

2.1.3. Robertson Method

Based on the method of Robertson & Wride (1998) [9], the cyclic strength ratio can be estimated using the following equation:

$$\text{Si } 50 \leq (qc1N) < 160: \quad CRR = 93 \left[\frac{(qc1N)_{cs}}{1000} \right]^3 + 0.08 \quad (10)$$

$$\text{Si } (qc1N) < 50: \quad CRR = 0.833 \left[\frac{(qc1N)_{cs}}{1000} \right]^3 + 0.05 \quad (11)$$

with $(1N)_{cs}$ the clean sand equivalent standardized penetration resistance calculated as follows:

$$(qc1N)_{cs} = Kc \, qc1N \quad (12)$$

- $qc1N$ is normalized penetration resistance, determined on the basis of the penetration resistance of the cone and corrected for the effective stress;
- Kc is a correction factor depending on the characteristics of the soil grains, which will be defined hereafter;
- I_c is the soil behavior type index;
- σ_v et σ'_v are both total and effective constraints;
- $Pa \, \sigma'_v$ is a pressure reference, has the same units as ($Pa = 100$ kPa if σ'_v expressed in kPa);
- $Pa2$ is a reference pressure has the same units as qc and σ_v ($Pa2 = 0.1$ MPa if qc e and σ_v are in MPa).

Figure 1 shows the flowchart of the research methodology through which the objectives of this study were achieved.

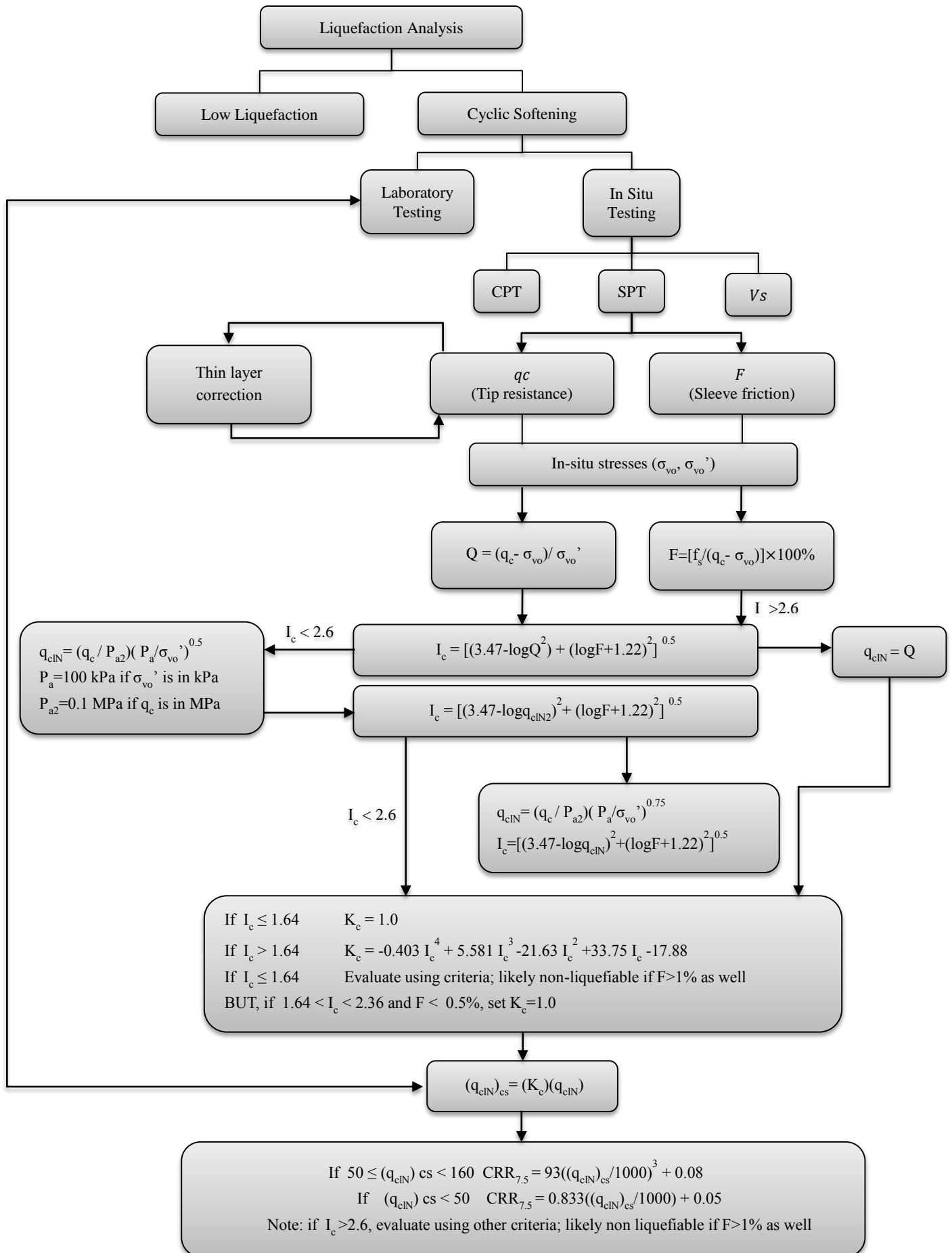


Figure 1. Method for evaluating Cyclic Resistance Ratio (CRR) [9]

2.2. Evaluating Cyclic Ratio Stress (CSR)

The cyclic stress ratio represents the average cyclic shear stress in a layer normalized to the vertical effective stress, this ratio is presented by Seed and Idriss 1971 [25] in following formula:

$$CSR = \tau_{avg} / \sigma'v = 0.65 (a_{max} / g) (\sigma_v / \sigma'v) rd \quad (13)$$

where τ_{avg} is the average cyclic shear stress in a normalized layer, $\sigma'v$ is the effective vertical stress, a_{max} is the maximum amplitude of the horizontal acceleration, g is the acceleration of gravity, σ_v is the total vertical stress from the weight of the overlying soils, and rd is the stress-reducing coefficient which is calculated as a function of depth by Liao and Whitman [26] using the following equations:

$$\begin{aligned} rd &= 1 - 0.00765 & Si : z \leq 9.15 \text{ m} & (24) \\ rd &= 1 - 0.00765 z & Si : 9.15 \text{ m} < z \leq 23 \text{ m} & \\ rd &= 0.744 - 0.008 z & Si : 23 \text{ m} < z \leq 30 \text{ m} & \\ rd &= 0.5 & Si : z > 30 \text{ m} & \end{aligned} \quad (14)$$

2.3. Evaluating Liquefaction Potential

The conditional probability of liquefaction at a site in each seismic event can be calculated (Juang et al. [7]) as follows:

$$PL = \frac{1}{1 + (F_s/A)^B} \quad (15)$$

where, A and B coefficients expressed for each method in Table 1.

Table 1. A and B according to the method used

Reference	A	B
Olsen (1997) [8]	1	2.78
Juang et al. (2003) [7]	0.96	4.50
Robertson & Wride (1998) [9]	1	3.30

Using the PL probability index, the occurrence of liquefaction can be ranked and analyzed based on the Table 2.

Table 2. Liquefaction occurrence based on probability index [27]

Probability index	Class	Liquefaction probability
$P_L \geq 0,85$	5	Liquefaction almost certain
$0,65 \leq P_L < 0,85$	4	Liquefaction very likely
$0,35 \leq P_L < 0,65$	3	Liquefaction and non-liquefaction are possible
$0,15 \leq P_L < 0,35$	2	Liquefaction unlikely
$P_L < 0,15$	1	Liquefaction almost impossible

3. Case Study

3.1. Geographic Location and Geological Context of the Study Area

Our case study is part of the compressible zone of the Oued Gharifa valley, with the aim of realizing the section from KP 228+400 to KP 229+400 of the high-speed line linking Tangier and Casablanca. Figure 2 represents a satellite view of our study area. The covering soils of the surrounding hills are Pliocene shell silts, with, at the foot of the slopes, colluvium from these terraces. From a structural point of view, the area is attached to the Habt nappe. It seems that the area is close to a contact between the pelites with rare sandstone turbidite beds of the middle Eocene to the Oligocene and the sandstone turbidites with marly beds of the Oligocene.

3.2. Soil Condition and Fact-Finding Mission at the Study Area (Description of the Geotechnical Longitudinal Profile)

Laboratory identification and characterization tests were carried out at different depths (up to 36m) on intact and reworked samples from the core borings. These surveys allowed the establishment of a detailed geotechnical profile represented as follows:

- At the end of the valley, precisely between KP228+460 to KP228+600, a slightly consistent clay is encountered, 5 to 7m thick, overlying the pelitic bedrock, which has a weathering fringe about 5 m thick,
- From KP 228+600 to KP 228+900, there is an appearance of mudstone formations, underlying beige clays and alluvium intercalated between the bedrock and the surface clay formation,

- From KP 228+900 to KP 229+300, a second zone of bedrock excavation appears with the disappearance of the altered fringe replaced by alluvial deposits,
- From KP 229+300, at the foot of the slope, sandy colluvium resting directly on the pelitic bedrock.

Another point is that several in-situ tests were done, including pressuremeter tests, dynamic penetrometer tests, scissometer tests, and static penetrometer tests, whose results have been used to evaluate the liquefaction risks (see Table 3).

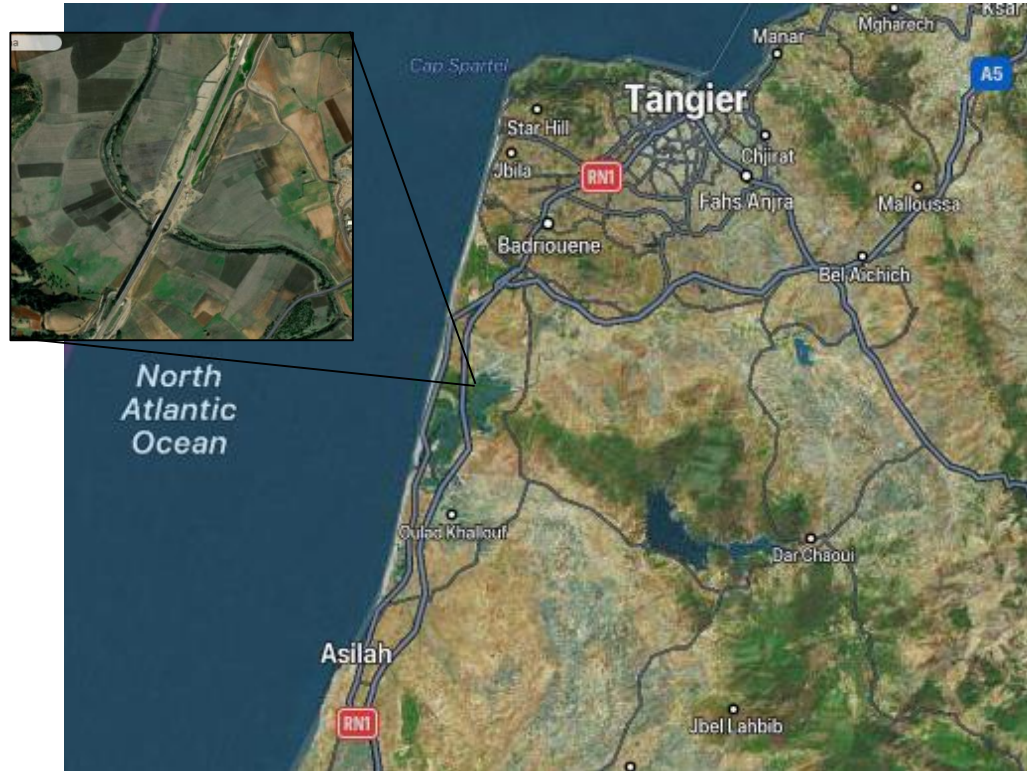


Figure 2. Satellite view of the studied site

Table 3. Mechanical and in-situ parameters of soil layers

Area	KP	Layer	Thickness (m)	Cu (kPa)	γ (Kn/m ³)	CPT			Scissor meter
						qc (MPa)	PI*(MPa)	E(MPa)	
Area 1	KP 228+600	Slightly Consistent Clay	6.5	48	20.8	1.5 - 3	0.65-1.05	3.6-35	85 to >9
		Pelitic Clay	5.5	110	19	15 - 2.5	1.2-3.1	4.8-110	-
		Grey Pelite	>5	-	-	-	>5	142- 545	-
Area 2	KP 228+860	Over-Consolidated Crust	2	50	20.8	1.5 - 3	0.65-1.05	3.6-35	85 to >9
		Slightly Consistent Clay	3	38	20.8	1.5 - 3	0.65-1.05	3.6-35	85 to >9
		Blackish Silt	3	29	19	0.4 – 0.7	0.111-0.34	0.15-1.9	32-51
		Beige Silty Clay	5	76	20.7	0.75 – 1.1	-	-	90
		Alluvium	2.5	-	20	4	-	7	-
		Pelitic Clay	4	110	19	1.5 – 2.5	1.2-3.1	4.8-110	-
		Grey Pelite	>5	-	-	-	>5	142- 545	-
Area 3	KP 229+120	Over-Consolidated Crust	2	50	20.8	1.5-3	0.65-1.05	3.6 - 35	85 to >9
		Slightly Consistent Clay	4.5	38	20.8	1.5-3	0.65-1.05	3.6 - 35	85 to >9
		Blackish Silt	6.5	29	29	0.4-0.7	0.111-0.34	0.15 – 1.9	32-51
		Alluvium	6	39	20	4	-	7	-
		Grey Pelite	>5	-	-	-	>5	142- 545	-
Area 4	KP 229+325	Beige Sand	1	-	19	4	-	-	-
		Slightly Consistent Clay	3	90	20.8	1.5-3	0.65-1.05	3.6 - 35	85 à >9
		Alluvium	3	-	20	4	-	7	-
		Grey Pelite	>5	-	-	-	>5	142- 545	-

3.3. Seismic Risk

According to RPS 2000 revised in 2011 [28], the valley of Oued Gharifa is part of the seismic zone N° 3, where the maximum horizontal acceleration of the ground $A_{max} = 14\%$ g and the maximum horizontal velocity of the ground $V_{max}=13$ cm/s (Figure 3).

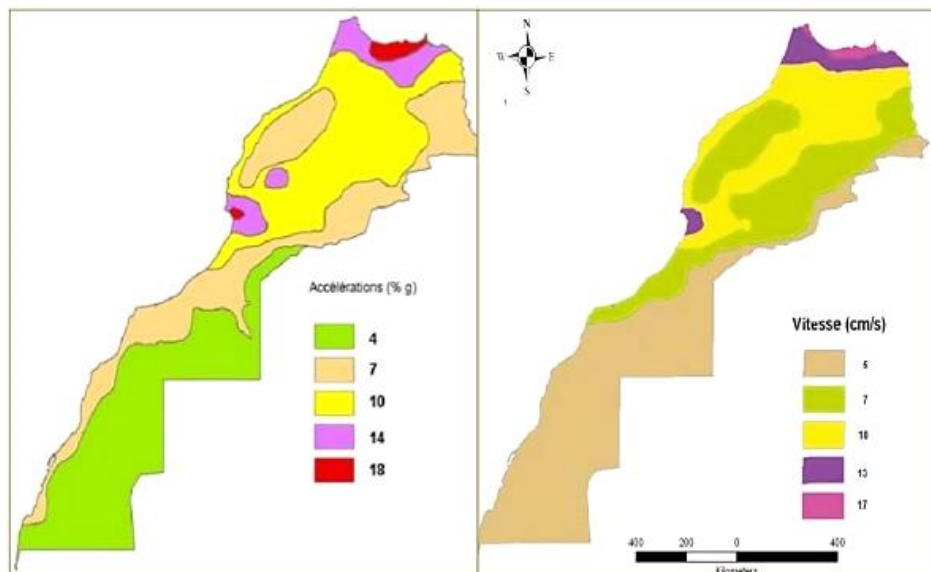


Figure 3. Seismic zoning in acceleration and velocity for probabilities of 10% in 50 years Morocco 2011

The valley of Oued Gharifa is characterized by a maximum intensity limited between VII and VIII, but for safety reasons (area near regions of high seismic intensity) we consider an intensity of IX that corresponds to a magnitude $M = 6.5$.

4. Results and Discussions

Given the data of the four CPT test surveys, we were able to evaluate the safety coefficient, as well as the liquefaction potential of the embankment crossing the Gharifa river valley, between KP228+400 and KP229+375. However, the evaluation of the liquefaction susceptibility of this compressible zone was established by three semi-empirical methods through cyclic stress approach (See results in Table 4).

4.1. Evaluating Liquefaction Potential

In analyzing the calculations based on the CPT test outputs and regarding the four surveys that used the three semi-empirical methods, we notice that:

- The survey undergone at KP 228+600 in the northern part of the valley shows low liquefaction potential due to the existence of clay layers less susceptible to liquefaction.
- The results in zone two at KP 228+860, indicate that the liquefaction potential is higher for the layers located between 8m and 12m. This susceptibility is mainly due to the existence of beige silty clays and alluvium characterized by a PL exceeding 0.5.
- Including all of the three methods, sector three at KP 229+120 is characterized by a low susceptibility to liquefaction for a depth greater than 13m. Conversely, the layers shaped by alluvium show a high PL.
- For the last area at KP 229+325, a high PL is observed for the depth of 0.1m to 1m and of 4m to 7m, due to the existence of a sandy formation of 1m thickness on the surface clays and alluvium constituting a layer of 3m thickness susceptible to liquefaction.

4.2. Comparison between Methods' Results

In this section, we compare the three semi-empirical methods of the more liquefaction-prone areas of the two boreholes at KP 228+860 and KP 229+325.

In the Figure 4, we notice the variation of safety factor at KP 228+860 where the depths of less than 4 have a FS less than 1m, which presents a susceptibility to liquefaction.

Table 4. In-situ characteristics

Area	KP	Depth (m)	Classification	Olsen method				Juang method				Robertson method			
				CRR	CSR	FS	PL	CRR	CSR	FS	PL	CRR	CSR	FS	PL
Area 1	KP 228+600	1	Slightly Consistent Clay	0.19	0.16	1.19	0.38	0.18	0.11	1.62	0.09	0.19	0.11	1.71	0.15
		2		0.16	0.17	0.94	0.54	0.12	0.12	1.02	0.44	0.13	0.12	1.10	0.42
		3		0.2	0.16	1.25	0.35	0.09	0.11	0.81	0.68	0.10	0.11	0.90	0.59
		4		0.14	0.15	0.93	0.55	0.15	0.10	1.44	0.14	0.16	0.10	1.54	0.20
		5		0.19	0.13	1.46	0.26	0.17	0.09	1.88	0.05	0.14	0.09	1.55	0.19
		7	0.3	0.2	1.50	0.24	0.16	0.14	1.15	0.31	0.20	0.14	1.44	0.23	
		8	0.31	0.21	1.48	0.25	0.2	0.15	1.37	0.17	0.30	0.15	2.06	0.08	
		9	0.28	0.18	1.56	0.23	0.21	0.13	1.68	0.07	0.19	0.13	1.52	0.20	
		10	0.2	0.13	1.54	0.23	0.18	0.09	1.99	0.04	0.18	0.09	1.97	0.10	
		11	0.23	0.16	1.44	0.27	0.17	0.11	1.53	0.11	0.17	0.11	1.49	0.21	
		Area 2	KP 228+860	1	Overconsolidated Crust	0.27	0.17	1.59	0.22	0.16	0.12	1.36	0.17	0.19	0.12
2	0.22			0.16		1.38	0.29	0.19	0.11	1.71	0.07	0.13	0.11	1.17	0.37
3	Slightly Consistent Clay			0.19	0.12	1.58	0.22	0.13	0.08	1.56	0.10	0.10	0.08	1.20	0.35
4				0.34	0.18	1.90	0.14	0.18	0.13	1.44	0.14	0.16	0.13	1.28	0.31
5				0.28	0.16	1.75	0.17	0.17	0.11	1.53	0.11	0.14	0.11	1.26	0.32
6	Blackish Sludge			0.33	0.18	1.83	0.16	0.192	0.13	1.54	0.11	0.20	0.13	1.60	0.17
7				0.23	0.18	1.29	0.33	0.18	0.13	1.44	0.14	0.23	0.13	1.84	0.12
8	0.33			0.18	1.82	0.16	0.15	0.13	1.20	0.27	0.19	0.13	1.52	0.20	
9	Beige Silty Clay			0.14	0.16	0.88	0.59	0.12	0.11	1.08	0.37	0.12	0.11	1.08	0.44
10				0.16	0.17	0.94	0.54	0.1	0.12	0.85	0.64	0.08	0.12	0.68	0.78
11				0.14	0.15	0.93	0.55	0.09	0.10	0.86	0.62	0.11	0.10	1.06	0.46
12				0.15	0.17	0.88	0.59	0.11	0.12	0.93	0.53	0.09	0.12	0.76	0.71
13				0.2	0.18	1.11	0.43	0.16	0.13	1.28	0.22	0.17	0.13	1.36	0.27
14				0.19	0.18	1.06	0.46	0.15	0.13	1.20	0.27	0.18	0.13	1.44	0.23
Area 3	KP 229+120	1	Overconsolidated Crust	0.21	0.19	1.14	0.41	0.15	0.13	1.12	0.33	0.17	0.13	1.33	0.28
		2		0.23	0.18	1.27	0.34	0.13	0.12	1.09	0.36	0.20	0.12	1.61	0.17
		3	Slightly Consistent Clay	0.21	0.15	1.37	0.30	0.12	0.11	1.16	0.30	0.12	0.11	1.16	0.38
		4		0.19	0.17	1.13	0.42	0.13	0.12	1.13	0.32	0.16	0.12	1.36	0.26
		5		0.24	0.16	1.50	0.25	0.15	0.11	1.34	0.18	0.13	0.11	1.17	0.37
		6		0.20	0.19	1.04	0.47	0.14	0.13	1.07	0.38	0.16	0.13	1.23	0.33
		9	Blackish Sludge	0.19	0.17	1.10	0.43	0.17	0.12	1.42	0.15	0.18	0.12	1.55	0.19
		10		0.22	0.16	1.36	0.30	0.14	0.11	1.23	0.25	0.12	0.11	1.09	0.43
		11		0.27	0.19	1.38	0.29	0.15	0.13	1.15	0.31	0.15	0.13	1.14	0.40
		12		0.12	0.10	1.18	0.39	0.10	0.07	1.42	0.15	0.10	0.07	1.40	0.25
		13		0.16	0.17	0.95	0.54	0.14	0.12	1.17	0.29	0.11	0.12	0.93	0.56
		15		0.15	0.13	1.09	0.44	0.08	0.09	0.89	0.59	0.08	0.09	0.89	0.60
		16		0.15	0.16	0.95	0.53	0.10	0.11	0.91	0.56	0.11	0.11	0.95	0.54
19	0.11	0.12	0.94	0.54	0.07	0.08	0.85	0.64	0.09	0.08	1.08	0.44			
Area 4	KP 229+325	0.5	Beige Sand	0.14	0.18	0.78	0.67	0.12	0.13	0.96	0.50	0.11	0.13	0.88	0.60
		1		0.18	0.20	0.90	0.57	0.13	0.14	0.94	0.53	0.13	0.14	0.94	0.55
		2	Slightly Consistent Clay	0.21	0.20	1.05	0.47	0.20	0.14	1.44	0.14	0.18	0.14	1.30	0.30
		3		0.23	0.19	1.21	0.37	0.18	0.13	1.36	0.17	0.22	0.13	1.67	0.16
		4		0.19	0.17	1.12	0.42	0.16	0.12	1.35	0.18	0.16	0.12	1.39	0.25
		6	Alluvium	0.13	0.15	0.87	0.60	0.09	0.10	0.86	0.62	0.08	0.10	0.77	0.70
		7		0.18	0.16	1.13	0.42	0.14	0.11	1.26	0.23	0.19	0.11	1.71	0.15

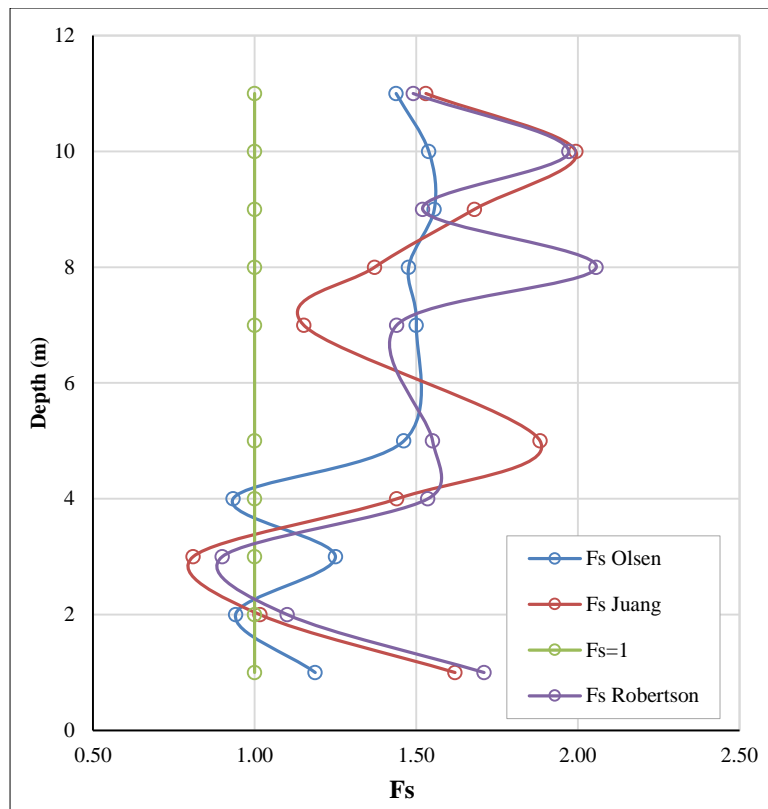


Figure 4. Fs KP 228+600

The variation of the FS curves is almost similar for the Juang and Robertson methods down to 4 m depth.

In Figure 5, we observe a discrepancy in variation of the CSR curves of the Olsen method and CSR of the other two methods, i.e. this discrepancy is mainly due to the introduction of the factor MSF in calculations of Juang method and Robertson method. This variation has an impact on the safety factor values though.

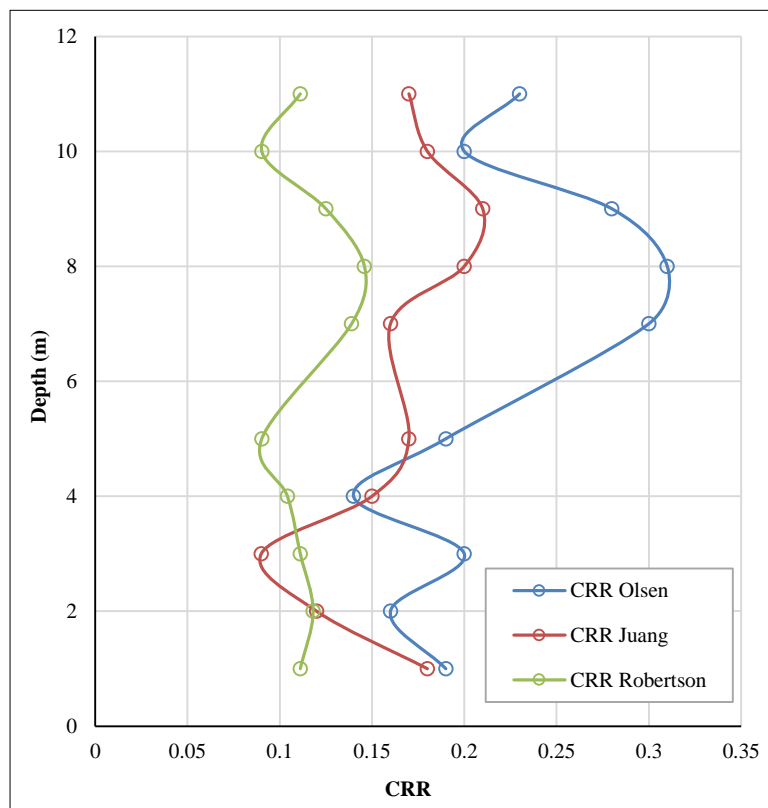


Figure 5. CSR KP 228+600

For a depth between 4m and 8m, we notice a difference between the variation curves of FS for Juang method and Robertson method to that of the Olsen method, this is mainly due to the variation of the CRR (Figure 6).

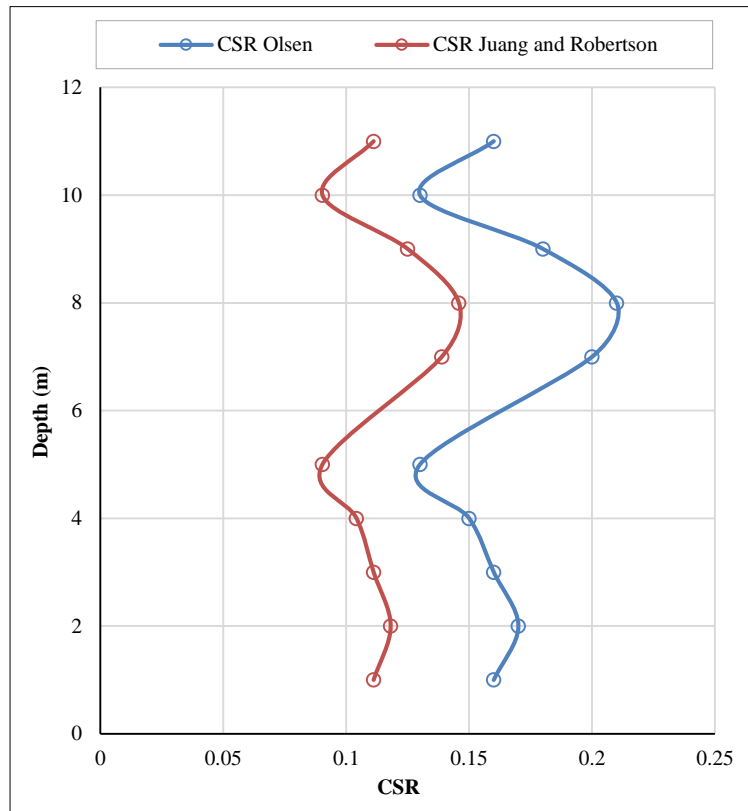


Figure 6. CRR KP 228+600

According to the analysis of the variation of the liquefaction potential in Figure 7, we find that the presented deviation is related to the change of the coefficients A and B depending on the method used. The three methods, however, show the same susceptibility of the layers to seismic stress.

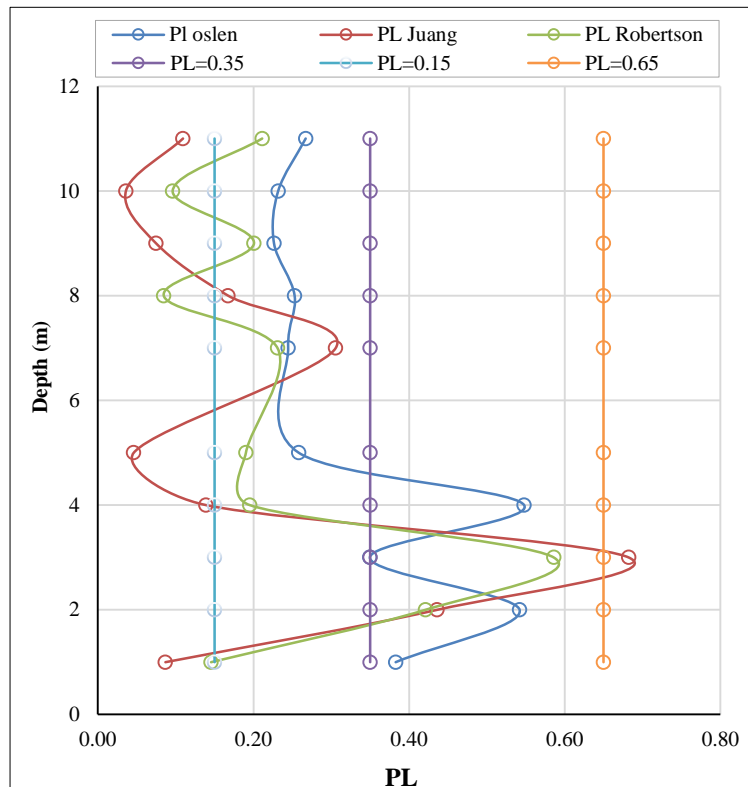


Figure 7. PL KP 228+600

Figure 8 illustrates the variation of the safety factor in the case KP 229+325, in which we notice the F_s is lower than 1. Also, it's clear that the variation of the F_s curves according to the three methods is almost similar at depths greater than 5 m.

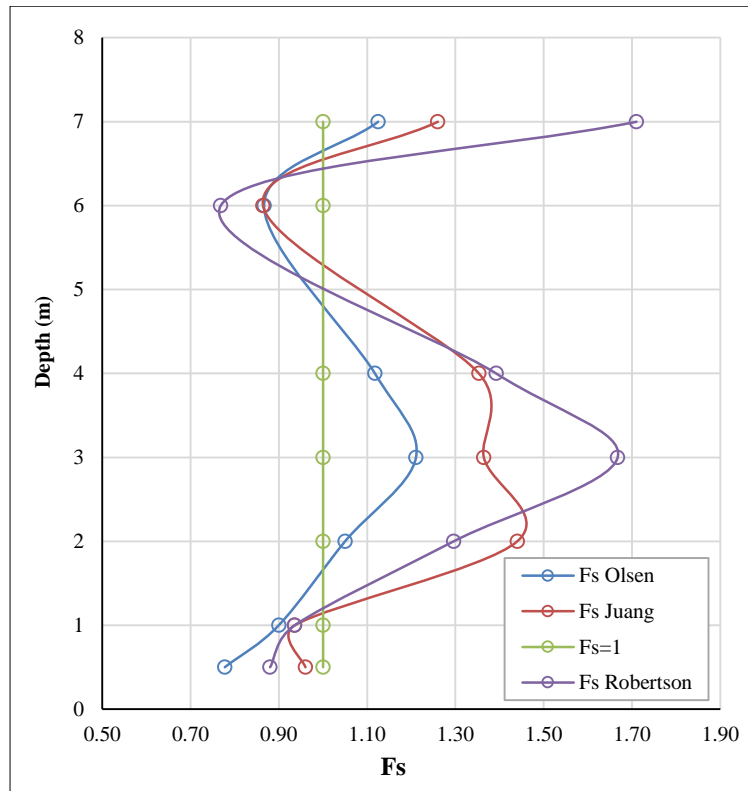


Figure 8. F_s KP 229+325

In contrast, the variation corresponding to the depths lower than 5m wherein we notice a difference between the curve of variation of the method of Olsen and the other two methods, this latter is due more particularly to the insertion of the factor MSF in the calculation of CSR in the method of Juang and that of Robertson (See Figures 9 and 10).

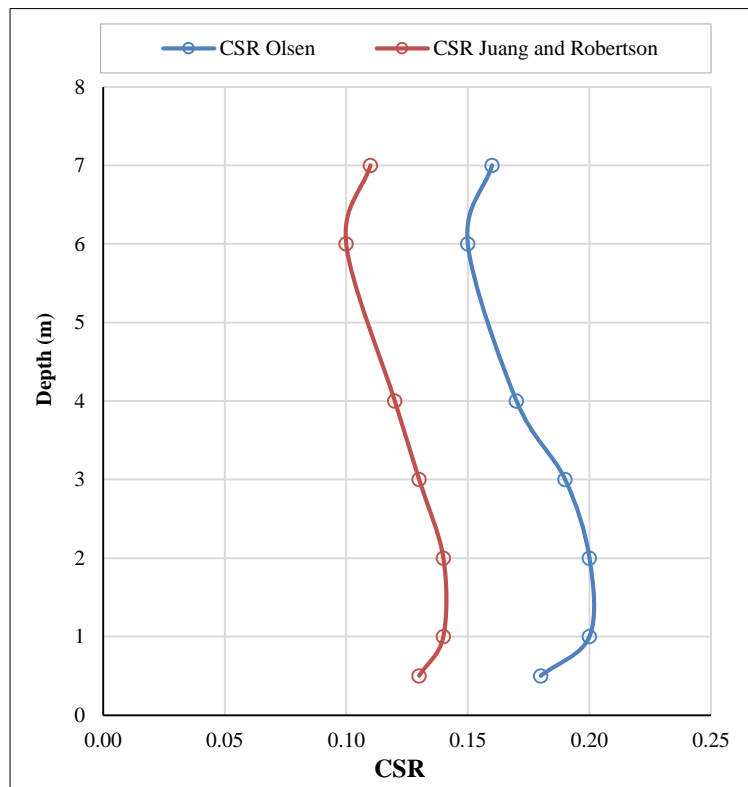


Figure 9. CSR KP 229+325

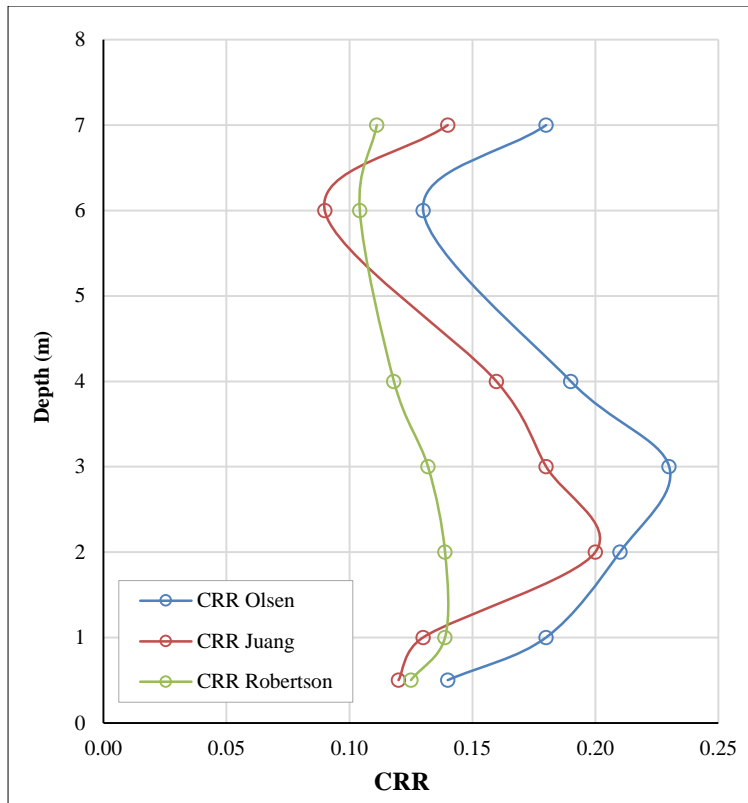


Figure 10. CRR KP 229+325

These analyses presented on the safety factor are directly projected on the variation of the liquefaction potential curves provided in Figure 11. The difference between the variation of PL and Fs is mainly related to the change of coefficients A and B from one method to the other.

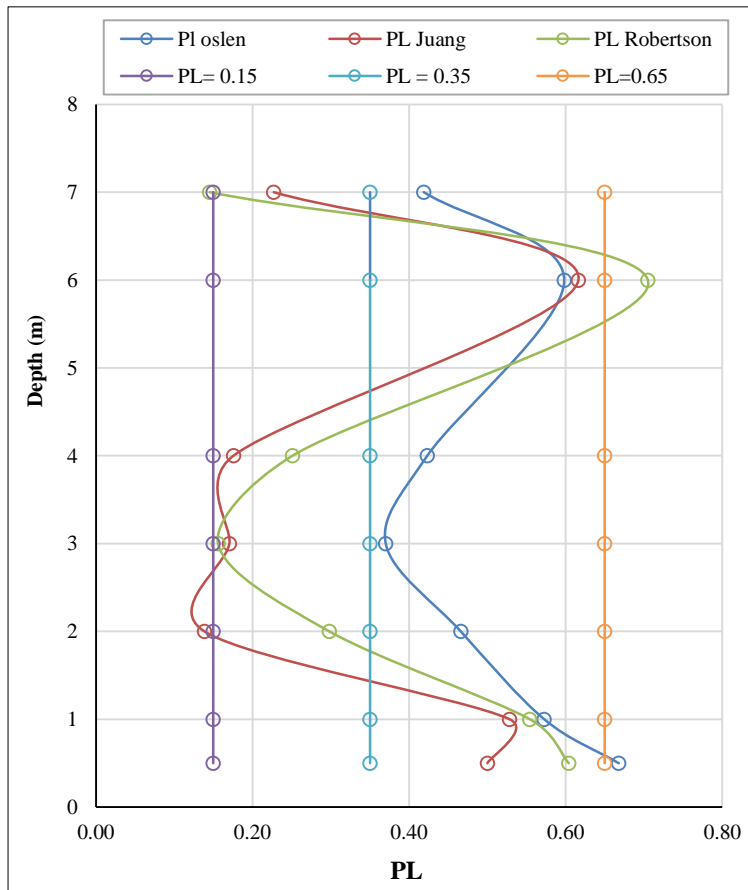


Figure 11. PL KP 229+325

Overall, with reference to the analysis of the different graphical illustrations of the liquefaction potential linked to the three methods used and for both of the selected profiles, we can deduce that the studied area presenting a PL between 0.15 and 0.35 corresponds to unlikely liquefaction, and a PL between 0.35 and 0.65 corresponds to a probability of liquefaction and not liquefaction under earthquake solicitations.

5. Conclusion

Since the Niigata and Alaska earthquakes in 1964, soil liquefaction has become the most interesting field of study in soil dynamics. As given earlier, a combination of a variety of factors should be available so that this phenomenon could take place. Firstly, the energy generated by the seism has to be sufficient. Secondly, the ground must be susceptible to liquefaction. Finally, a situation of underwater saturation should exist. If these conditions are present at a given site, liquefaction will be initiated, and consequently, its effects, such as boiling and slumping, will be a distinct indicator of its extent and severity.

Broadly speaking, many research studies have been developed in this regard with the intention of determining the potential of liquefaction. In this paper, the estimation of the liquefaction potential of soils in the compressible zone along Oued Gharifa was done using three semi-empirical methods based on the cyclic stress approach: the Olsen method, the Robertson method, and the Juang method. The data used to estimate the liquefaction potential of the section of the high-speed line from KP 228+400 to KP 229+375 are believed to be the outputs of the CPT tests.

We were able to verify the liquefaction susceptibility of the study area as well as compare the variation of the safety coefficient and the liquefaction potential for each method. Comparing the different methods used, we can conclude that the Juang method remains the most adapted and the most robust compared to the two other methods, mainly the Robertson method, which requires the intervention of several corrections. Finally, we can consider that the clays and muds shaping the northern part of the valley of Oued Gharifa are not liquefiable, unlike the foot of the slope, which is characterized by the existence of sandy colluvium resting directly on the pelitic bedrock and which has a high potential for liquefaction.

6. Declarations

6.1. Author Contributions

Conceptualization, F.E.L.; methodology, F.E.L., K.B., G.A., and L.E.; software, F.E.L.; validation, F.E.L., K.B., G.A., and L.E.; formal analysis, F.E.L.; investigation, F.E.L., K.B., G.A., and L.E.; resources, K.B.; data curation, F.E.L.; writing—original draft preparation, F.E.L.; writing—review and editing, F.E.L., K.B., G.A., and L.E.; visualization, K.B.; supervision, K.B. All authors have read and agreed to the published version of the manuscript.

6.2. Data Availability Statement

The data presented in this study are available in the article.

6.3. Funding

The authors received no financial support for the research, authorship, and/or publication of this article.

6.4. Conflicts of Interest

The authors declare no conflict of interest.

7. References

- [1] Niigata earthquake of 1964. (1998). Japan National Committee on Earthquake Engineering, Tokyo, Japan. Available online: https://www.iitk.ac.in/nicee/wcee/article/vol3_S-78.pdf (accessed on January 2023).
- [2] Kishida, H. (1966). Damage to Reinforced Concrete Buildings in Niigata City with Special Reference to Foundation Engineering. *Soils and Foundations*, 6(1), 71–88. doi:10.3208/sandf1960.6.71.
- [3] Walsh, T. J., Combellick, R. A., & Black, G. L. (1995). Liquefaction features from a subduction zone earthquake: preserved examples from the 1964 Alaska earthquake. Division of Geology and Earth Resources, Washington State Department of Natural Resources, Washington, United States.
- [4] Ishibashi, I., & Zhang, X. (1993). Unified dynamic shear moduli and damping ratios of sand and clay. *Soils and Foundations*, 33(1), 182–191. doi:10.3208/sandf1972.33.182.
- [5] Dobry, R., & Ladd, R. S. (1980). Discussion of “Soil Liquefaction and Cyclic Mobility Evaluation for Level Ground during Earthquakes and Liquefaction Potential: Science versus Practice.” *Journal of the Geotechnical Engineering Division*, 106(6), 720–724. doi:10.1061/ajgeb6.0000984.
- [6] Nemat-Nasser, S., & Shokooh, A. (1979). A unified approach to densification and liquefaction of cohesionless sand in cyclic shearing. *Canadian Geotechnical Journal*, 16(4), 659–678. doi:10.1139/t79-076.

- [7] Juang, C. H., Yuan, H., Lee, D.-H., & Lin, P.-S. (2003). Simplified Cone Penetration Test-based Method for Evaluating Liquefaction Resistance of Soils. *Journal of Geotechnical and Geoenvironmental Engineering*, 129(1), 66–80. doi:10.1061/(asce)1090-0241(2003)129:1(66).
- [8] Olsen, R. S. (1997). Cyclic liquefaction based on the cone penetrometer test. *Proceedings of the NCEER Workshop on Evaluation of Liquefaction Resistance of Soils*, 225-276, 5-6 January, 1996, State University of New York, Buffalo, United States.
- [9] Robertson, P. K., & Wride, C. (1998). Evaluating cyclic liquefaction potential using the cone penetration test. *Canadian Geotechnical Journal*, 35(3), 442–459. doi:10.1139/t98-017.
- [10] Idriss, I. M., & Boulanger, R. W. (2006). Semi-empirical procedures for evaluating liquefaction potential during earthquakes. *Soil Dynamics and Earthquake Engineering*, 26(2–4), 115–130. doi:10.1016/j.soildyn.2004.11.023.
- [11] Youd, T. L., & Idriss, I. M. (2001). Liquefaction Resistance of Soils: Summary Report from the 1996 NCEER and 1998 NCEER/NSF Workshops on Evaluation of Liquefaction Resistance of Soils. *Journal of Geotechnical and Geoenvironmental Engineering*, 127(4), 297–313. doi:10.1061/(asce)1090-0241(2001)127:4(297).
- [12] Latifi, F. E., Baba, K., Bahi, L., Touijrate, S., & Cherradi, C. (2020). Semi-empirical method for evaluating risk of liquefaction during earthquakes a study case of rhiss dam. *E3S Web of Conferences*, 150, 100. doi:10.1051/e3sconf/202015001004.
- [13] Touijrate, S., Baba, K., Ahatri, M., Bahi, L. (2019). The Liquefaction Potential of Sandy Silt Layers Using the Correlation Between Penetrometer Test and SPT Test. *Dynamic Soil-Structure Interaction for Sustainable Infrastructures, GeoMEast 2018. Sustainable Civil Infrastructures*. Springer, Cham, Switzerland. doi:10.1007/978-3-030-01920-4_2.
- [14] Touijrate, S., Baba, K., Ahatri, M., & Bahi, L. (2018). Validation and Verification of Semi-Empirical Methods for Evaluating Liquefaction Using Finite Element Method. *MATEC Web of Conferences*, 149, 02028. doi:10.1051/mateconf/201814902028.
- [15] Olsen, R. S. (1984). Liquefaction analysis using the cone penetrometer test. *Proceedings of the 8th World Conference on Earthquake Engineering*, 247-254, San Francisco, United States.
- [16] Bouafia, A. (2011). *In situ tests in foundation projects (3rd Ed.)* OPU editions, University Publications Office, Algiers, Algeria.
- [17] Lankelma G.Z. (2023). Les spécialistes du pénétromètre statique. Available online: <http://www.lankelma.fr/penetrometre.html> (accessed on January 2023).
- [18] Zhang, L., Peng, Y., & Yang, J. (2019). Transformation of dissolved organic matter during advanced coal liquefaction wastewater treatment and analysis of its molecular characteristics. *Science of the Total Environment*, 658, 1334-1343. doi:10.1016/j.scitotenv.2018.12.218.
- [19] Park, T., So, S., Jeong, B., Zhou, P., & Lee, J. U. (2021). Life cycle assessment for enhanced Re-liquefaction systems applied to LNG carriers; effectiveness of partial Re-liquefaction system. *Journal of Cleaner Production*, 285, 124832. doi:10.1016/j.jclepro.2020.124832.
- [20] Seed, H. B., & Idriss, I. M. (1971). Simplified Procedure for Evaluating Soil Liquefaction Potential. *Journal of the Soil Mechanics and Foundations Division*, 97(9), 1249–1273. doi:10.1061/jsfeaq.0001662.
- [21] Hossain, M. B., Roknuzzaman, M., & Rahman, M. M. (2022). Liquefaction Potential Evaluation by Deterministic and Probabilistic Approaches. *Civil Engineering Journal*, 8(7), 1459-1481. doi:10.28991/CEJ-2022-08-07-010.
- [22] Harder Jr, L. F., & Boulanger, R. (1997). Application of K and K correction factors. *Proceedings of the NCEER Workshop on Evaluation of Liquefaction Resistance of Soils*, 225-276, 5-6 January, 1996, State University of New York, Buffalo, United States.
- [23] Rolsen, R. S., Koester J. P., & Hynes, M. E. (1996). Evaluation of liquefaction potential using CPT. *Proceedings of the 28th joint meeting of the US-Japan cooperative Program in natural resources - Panel on Wind and seismic effects*, Us national Institute of standards and technology, 14-17 May, 1996, Gaithersburg, Maryland, United States.
- [24] Wei, Y., Fakudze, S., Yang, S., Zhang, Y., Xue, T., Han, J., & Chen, J. (2023). Synergistic citric acid-surfactant catalyzed hydrothermal liquefaction of pomelo peel for production of hydrocarbon-rich bio-oil. *Science of The Total Environment*, 857, 159235. doi:10.1016/j.scitotenv.2022.159235.
- [25] Seed, H. B. (1982). *Ground motions and soil liquefaction during earthquakes*. Earthquake Engineering Research Institute, Oakland, United States.
- [26] Liao, S. S., & Whitman, R. V. (1986). *A catalog of liquefaction and non-liquefaction occurrences during earthquakes*. Department of Civil Engineering, Massachusetts Institute of Technology, Cambridge, United States.
- [27] Chen, C. J., & Juang, C. H. (2000). Calibration of SPT- and CPT-Based Liquefaction Evaluation Methods. *Innovations and Applications in Geotechnical Site Characterization, Geo-Denver 2000*, 49-64. doi:10.1061/40505(285)4.
- [28] Du Maroc, R. (2001). *The Seismic Construction Regulations*. Report RPS2000, Ministry of ATUHE, State Secretariat for Housing, Rabat, Morocco.